2017-01-01

Air permeability of balsa core, and its influence on defect formation in resin infused sandwich laminates

Cullen, Richard

ICCM International Conferences on Composite Materials

AIR PERMEABILITY OF BALSA CORE, AND ITS INFLUENCE ON DEFECT FORMATION IN RESIN INFUSED SANDWICH LAMINATES

Richard K. Cullen[1], Stephen M. Grove[1] and John Summerscales[1]

[1] School of Engineering, Plymouth University, Plymouth PL4 8AA, United Kingdom,
R.Cullen@plymouth.ac.uk, https://www.fose1.plymouth.ac.uk/sme/acmc

Keywords: Balsa, Core materials, Resin Infusion, RIFT

ABSTRACT

Many large composite structures are manufactured using sandwich laminates to achieve high specific bending strength and stiffness. For wind turbine blades, the self-weight becomes increasingly important as blade size increases. Resin infusion of three-dimensional sandwich laminates can result in complex flow paths, and subsequent defect formation is difficult to predict. The core material used for sandwich construction and its interaction with liquid resins may also influence the formation of defects. In the case of balsa, this effect can be used to reduce defect severity.

This paper considers the effect of cored sandwich laminate construction on the formation of defects. The primary focus is the characterisation of commonly used core materials and their interaction with liquid resin under high vacuum conditions. For balsa core, experiments indicate that the available pore space can act as a sink for trapped air, which can aid the reduction of defects when multiple flow fronts converge due to the complex flow paths in sandwich laminates. Empirical data for air absorption and desorption rates in balsa core were obtained using a custom-designed experiment.

Using these data, a theoretical model was developed that can indicate available pore space, which in turn informs optimum processing conditions, such as time under vacuum. The diffusion coefficients obtained for air absorption and desorption in balsa are very similar, and lie in the middle of published ranges for hard woods at around 2 x 10^{-7} m^2/s. The methodology developed represents actual behaviour of air absorption/desorption during resin infusion, whilst other techniques do not, merely measuring diffusion of air through a sample while not allowing for finite pore space. In consequence, infusion strategies can be planned more precisely because the core/resin interaction is better understood. Knit line defect formation could be predicted with greater accuracy with suitably modified flow-modelling programs.

1 INTRODUCTION

In nature, lightweight structures are often comprised of a compliant cellular or honeycomb core to increase buckling resistance with stiff, strong outer skins for flexural stiffness [1]. High-performance composites use a similar concept with aramid-, carbon-, or glass fibre skins over a polymeric foam or aramid honeycomb [2]. There is increasing interest in the use of renewable materials in composite structures including natural fibre reinforcements, bio-based resins and/or natural core materials (balsa [3] and cork [4, 5]).

The manufacture of large composite structures, e.g. wind turbine blades or marine vessels, was traditionally undertaken by hand lamination, but has recently become dominated by resin infusion under flexible tooling with a flow medium (RIFT II, also known as SCRIMP or VARTM) [6-8]. Cullen [9] analysed the many and various forms of defect occurring during manufacture of commercial RIFT components and identified many potential defects. The major issues included surface depressions, fabric wrinkling, print-through, pin-holes, dry patches and voids or related defects. The principal forms of defects were aerated resin, milky laminates and knit lines.

Flow in cored laminates (reinforcement fabrics with, possibly multiple, core types is complex and hence difficult to predict. In manufacture by RIFT II, resin is fed from a distribution mesh on one face, through holes in the core, to feed the opposite face. For a regular array of through-core holes, the flow on the reverse side will be a series of expanding circles. Ideally, the flow from row (*n-1*) should pass the *n*th hole before it is fed from the obverse face. Otherwise, convergent flow fronts can lead to

residual air being compressed between the converging flow fronts and consequent "lock-off" defects. This paper considers the issues arising from the use of balsa wood as a core material in resin infused laminates and seeks to quantify the resin/core interactions through a series of experiments under varying processing parameters.

2 EXPERIMENTAL METHODOLOGY

Experiments were conducted using unsealed Baltek AL600 end-grain balsa samples (40 x 40 x 30 mm). Thirty samples were dried for 48 h at 103°C as per ISO 3130 [10]. After storage in a holding desiccator, they were weighed and the density calculated. The samples were then exposed to ambient conditions (20°C, 42% RH) for 48 h and then re-dried for four days. Similar experiments were conducted on three larger (60 x 60 x 25 mm) samples for moisture absorption over 40 h.

The 30 samples were wrapped in infusion mesh and immersed/weighted in 8 L of water in a vacuum pot. The chamber was evacuated to 80 mbar absolute for 100 h (lower absolute pressure caused the water to boil). The samples were then dried of excess surface water, weighed, then re-dried. Resin penetration experiments were conducted using a proprietary epoxy resin.

End grain balsa can absorb or release air during resin infusion. The rate at which this occurs may be critical in composite manufacturing, especially if the timescale is longer than that of the commercial process. A two-chamber apparatus was developed with a 1.5 l sample (six cylindrical pieces) sensibly filling one chamber connected to a 2.5 l reservoir. SDX 15D4 pressure sensors were used in both chambers and a Digitron 2085P digital pressure gauge on the vacuum line. Diffusion coefficients were determined based on a modification of the Carslaw and Jaeger [11] classical solution for heat transfer.

Comparative tests were run with impermeable acrylic sheet or balsa core to examine the effect of core porosity on the presence of knit lines in a 150 mm square model laminate. The experimental rig produced four separate glycerol flow fronts from holes near the corners of the core, with flow converging to the centre of the plate.

Subsequent infusion experiments were conducted with EBX936 non-crimp glass fabric and the proprietary epoxy resin. Five core materials were used: (i) unsealed 130 kg/m^3 Baltex AL600 balsa (ii) sealed 150 kg/m^3 Baltex AL600T balsa, (iii) Fagerdala 150 kg/m^3 PET foam, (iv) 60 kg/m^3 Airex T90.60 PVC foam, and (v) 1180 kg/m^3 Perspex poly(methylmethacrylate (PMMA) solid as a non-permeable reference panel. A square grid of 3 mm flow holes were drilled through the core with either 25mm or 40 mm spacing. A high flow distribution medium was used to ensure that flow through the laminate thickness would be virtually simultaneous for all samples.

3 RESULTS

The initial average density of the small samples was 119 kg/m^3 and average moisture uptake was 6.7% by weight. The sample masses after re-drying were marginally lower (within the boundaries of experimental error) than after initial drying. The average moisture uptake for the three larger samples was 7.4% by weight (Fig. 1). The rate of moisture absorption was quite rapid, with 50% of the final level reached in the first 100 minutes of the experiment.

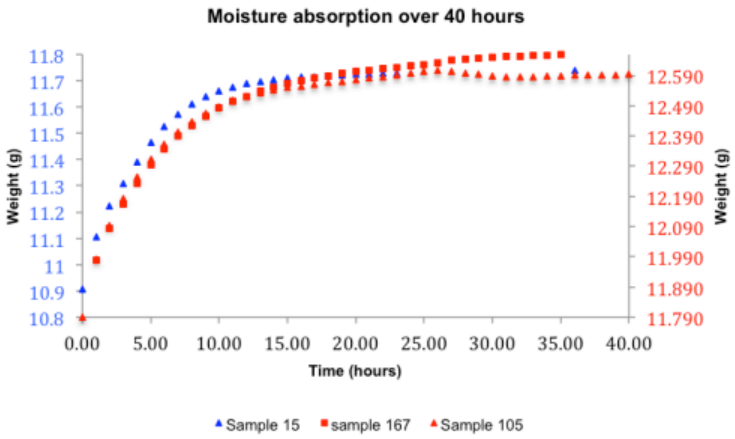

Fig. 1: Weight gain due to moisture absorption for three samples of AL600T end grain balsa.

The samples exposed to water under vacuum had percentage weight increases of 300-500% with a trendline indicating lower absorption in higher density samples. A single sample immersed in dilute black dye, then sectioned, indicated a penetration depth of 500 μm parallel to the grain direction/sap channels and no detectable penetration transverse to the grain. The resin experiments revealed penetration depths between 250-500 μm.

In the air absorption experiments, a stable 676 mbar absolute pressure was achieved after 1350 minutes. In 1000 minute tests, equalisation of the chamber pressures was at 328 mbar for desorption and at 320 mbar for absorption (Figs. 2-3). Experiments were conducted with half the balsa discs replaced by (notionally impermeable) PTFE discs. The pressure changes were close to half for the experiments with PTFE discs included.

Using the data from the final (680th) data point of each experiment, the balsa pore space was calculated to be in the ranges 69-84% for desorption and 65-78% for absorption (each based on three experiments) with high density samples having low pore space and *vice versa*.

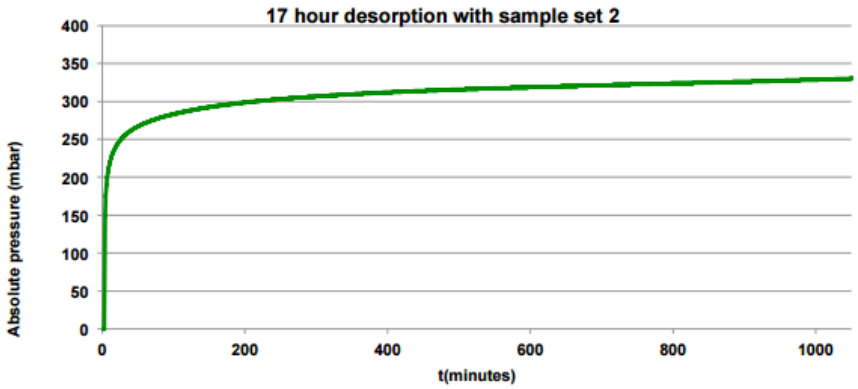

Fig. 2: 17-hour desorption run to provide comparison between absorption and desorption RH 53%, P 999 mbar, T 21ºC.

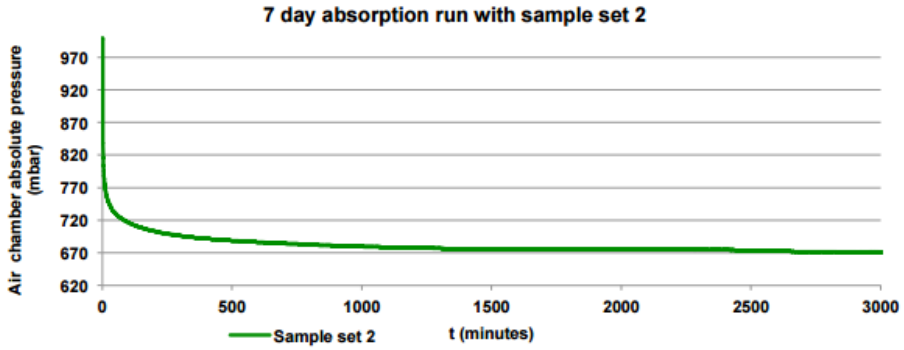

Fig. 3: Seven-day absorption to determine equalisation pressure, and leak rate.
RH 47%, P 337 mbar, T 22ºC.

Experimental and theoretical data for the diffusion coefficient are shown in Figure 4. The first 90 seconds of experimental data were not used, to eliminate the effect of free air movement, which the model does not simulate. The thermal analogy model (air supply ≡ heat source, and pressure ≡ temperature) is required to represent conditions where the source is finite and reduces over time, and the solid has a finite heat capacity. An approximate diffusion coefficient of $1x10^{-4}$ m^2 /s was obtained.

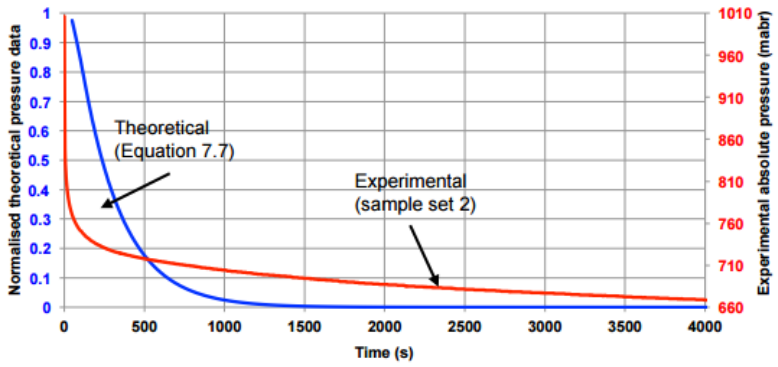

Fig. 4: Comparison of the theoretical (thesis equation 7.7) and experimental absorption data.

The flow fronts from the comparative tests are shown in Fig. 5. The reinforcement was 350 gm^{-2} Unifilo continuous random swirl filament mat. Clearly, the impermeable core produces a large unwetted region while there is full fill with the permeable balsa core.

Fig. 5: Comparative stalled flow positions on the reverse face
for acrylic (left) and balsa (right) cores.

In the infusion experiments, the spacing of the flow holes made little difference to the fill times. Knit lines were present where fibre tows did not fully wet-out leaving partially impregnated fabric where residual gases are compressed preventing resin from fully filling the region of convergence (Fig. 6). The unsealed balsa produced notionally defect free panels, while the PET and acrylic cores had poor laminate quality. When balsa is used as the core, as the air is compressed by the advancing flow front it can be absorbed by the core material with consequent elimination of the defects.

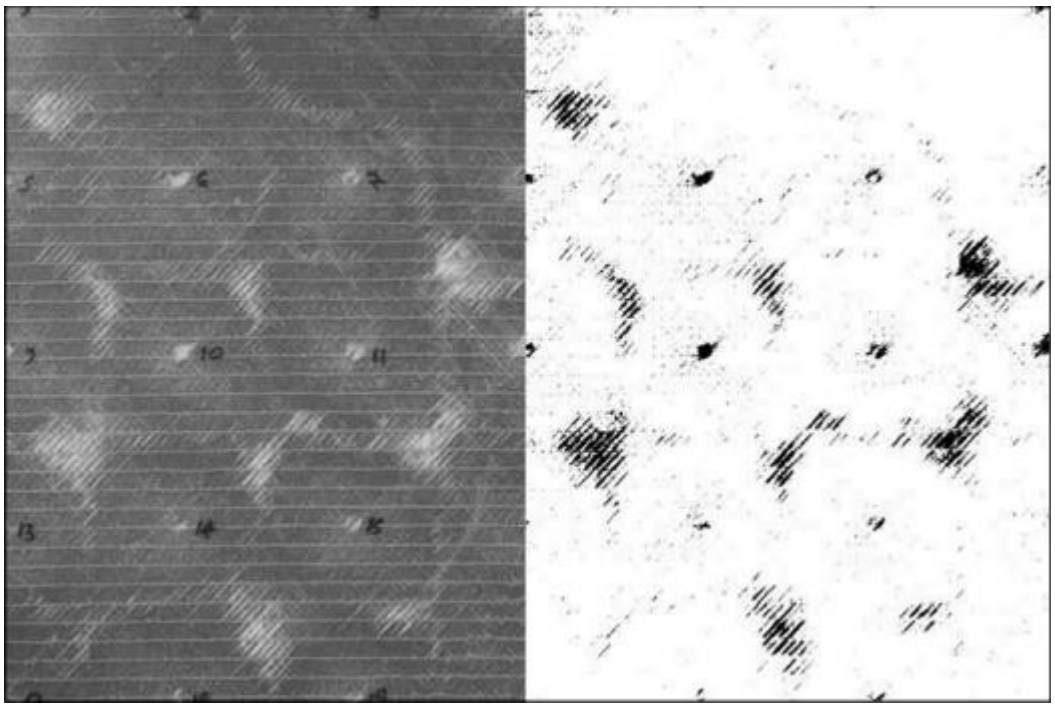

Fig. 6: Dry patches between convergent flow fronts from multiple holes in the core material.
Left: optical image of experimental sample,
Right: binary image to emphasis unwetted regions (black).

Table 1 presents summary data for the four panels analysed. Each image was analyed five times to minimise the effect of errors. Sealed and unsealed balsa show low knit line formation with significantly higher resin absorption, while closed cell PVC and PET foams have significant knit line production with low resin absorption.

	25 mm grid spacing				40 mm grid spacing			
	US balsa	Balsa	PVC	Acrylic	US balsa	Balsa	PVC	Acrylic
Expt. 1 (%)	0.1	0.2	2.4	6.6	0.6	0.8	2.1	4.4
Expt. 2 (%)	0.2	0.1	2.9	6.7	0.3	0.1	2.1	5.6
RA (kg m^{-3})	2.5	1.9	1.0	~~	2.4	2.1	0.9	~~

Table 1: Knit-line percentage from surface area measurements, and resin absorption (RA) (US = unsealed).

4 MODELLING

Resin flow through fibre preforms can be considered as equivalent to an incompressible fluid flow through a porous medium. 2D modelling of the fill phase during a liquid resin infusion process is based on incompressible mass conservation. Standard assumptions are Newtonian fluids, and negligible inertia and gravity effects. Flow modelling experiments have demonstrated that Darcy's law can be used over the range of flow rates and pressures used in liquid composite moulding. In resin infusion under flexible tooling, the cavity height is a time-dependent function of the fabric compressibility (not modelled here).

PAM-RTM (non-conforming finite element approximation: ESI Group/France) and Liquid Injection Moulding Simulation (LIMS finite element/control volume method with LEGO command line model generator: University of Delaware/USA) were used to investigate their respective abilities to predict flow front convergence zones, and subsequent resin lock-off. For cored laminates, complex 3D flow creates opportunities for air interchange with the core, rather than air being compressed when fluid fronts converge.

PAM-RTM was unable to deal with two-phase flow, which limits the effectiveness of the simulation, as air drawn into a porous core was not simulated.

The LIMS software was benchmarked against a simple infusion experiment. A rectangular laminate (500 x 50 mm) with eight layers of 290 gm^{-2} Unifilo U813-300 continuous random swirl E-glass fibre mat was infused with Sicomin SR8100/SD8724 epoxy resin system at a pressure differential of 996 mbar (7 mbar absolute in the bag) and ambient temperature. The cured plate was 3.7 mm thick with a fibre volume fraction of 24.6%. The experimental fill time was 203 s while, using a permeability of 750 x 10^{-12} m^{-2} for the reinforcement at 25% fibre volume fraction [12], Darcy's equation predicted 202 s and converged LIMS predicted 204 s demonstrating that the modelling was fundamentally sound.

Unlike PAM-RTM, LIMS must have an absolute pressure within the mould cavity defined for a simulation. The prediction of lock-off was sensitive to the mesh density used. Figure 7 shows that reasonably close convergence is achieved by 1600 elements (when modelling a theoretical 4% area lock-off). Full convergence required 22500 elements.

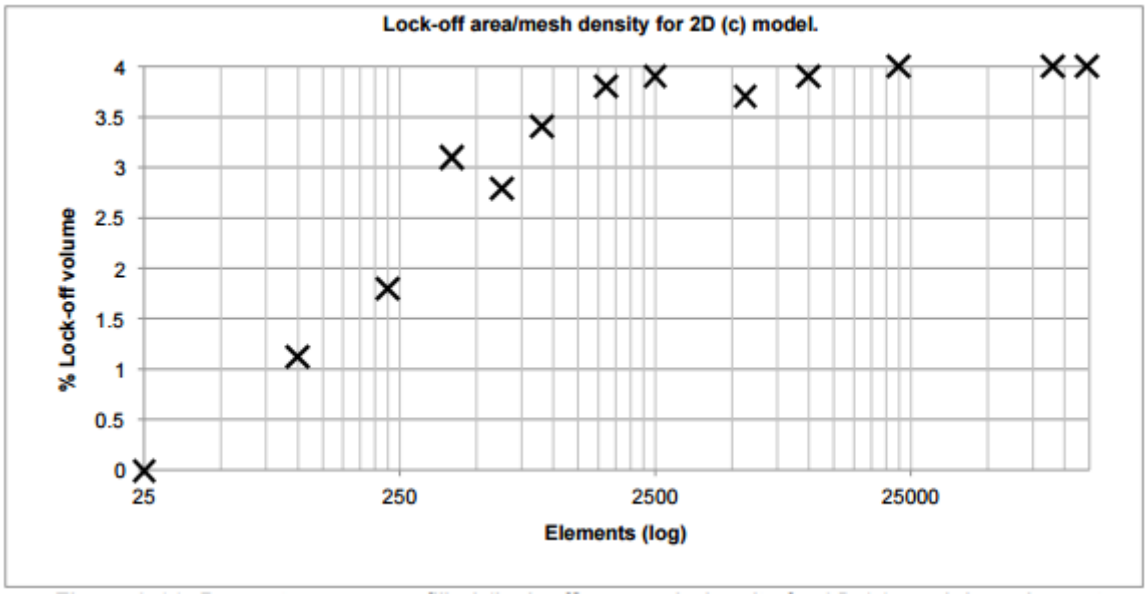

Figure 7: Unfilled area (5 lock-off) versus mesh density.

A reference model used 1568 2D elements representing the upper and lower skins. The bag-side skin permeabilities were representative of a plain-weave fabric combined with a flow medium, whereas the mould side skin had the permeability for plain-weave fabric alone. A central flow hole was represented by 1D bar elements. The benchmark model predicted lock-off at the four corners on the opposite face to the inlet when started with 40 mbar residual pressure, or no lock-off with full vacuum in the cavity.

A second model used 4333 elements in a similar configuration with 1D elements attached to each 2D nodal point to represent porosity in the core material. The model used four 1D elements to represent tow porosity at each nodal point of the 2D skins to model the impact of capillary pressure on air entrapment [149]. This model was capable of simultaneously modelling multi-scale (macro- and micro-) flow but proved to be complex and was abandoned.

5 BALSA AS A RESIN SINK

Figure 8 shows the experimental apparatus built to establish absorption/desorption rates in/from core materials [9]. An initial series of experiments were conducted to establish any equipment leak rate (measured over 7 days), baseline absorption/desorption levels, and absorption/desorption dependencies on core material volume. Absorption and desorption runs were conducted using tightly-fitting discs of unsealed AL600 end grain balsa from a single panel.

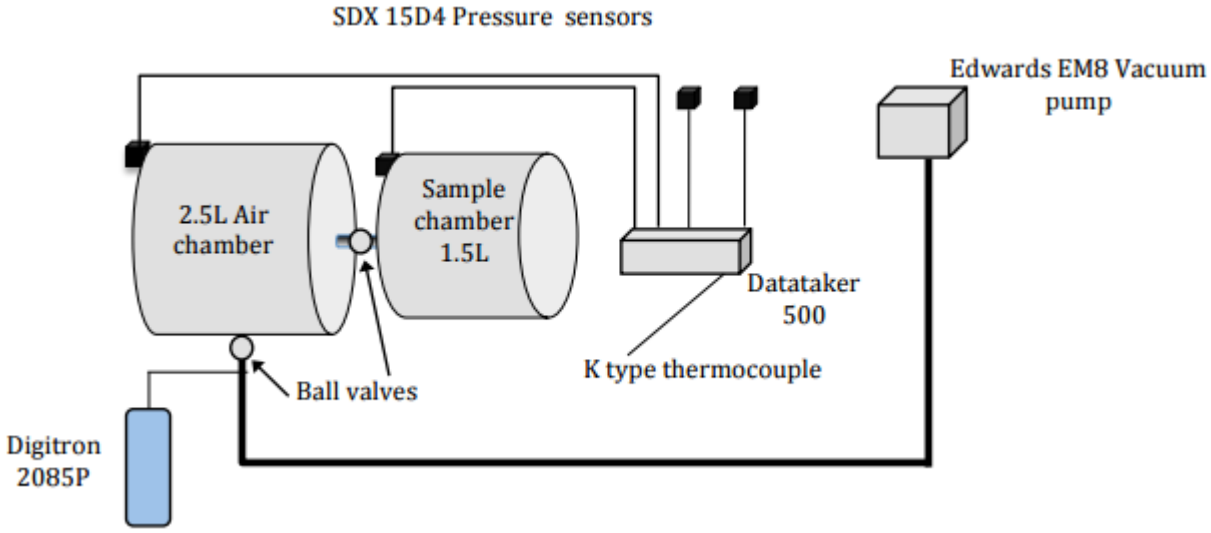

Figure 8: Schematic diagram of the experimental apparatus for absorption/desorption experiments

Fig. 9 and Fig.10 show the average absorption and desorption curves respectively for three samples. The small differences between absorption and desorption behaviour can be explained by the different ambient pressures at experiment start (~10 mbar), and the fact that balsa is a variable natural material making it susceptible to ambient condition fluctuations. 'Apparent' diffusion is comprised of two components of resistance to diffusion: external surface resistance and internal resistance.

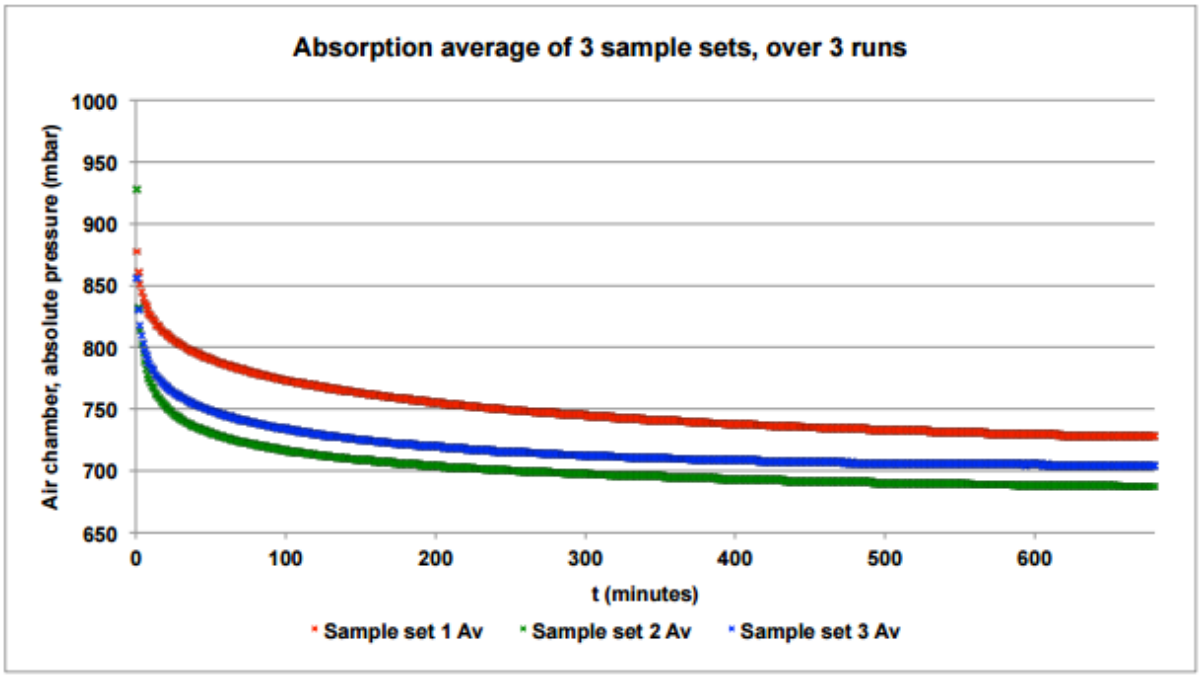

Figure 9: Absorption comparison of three sample sets with differing bulk densities.

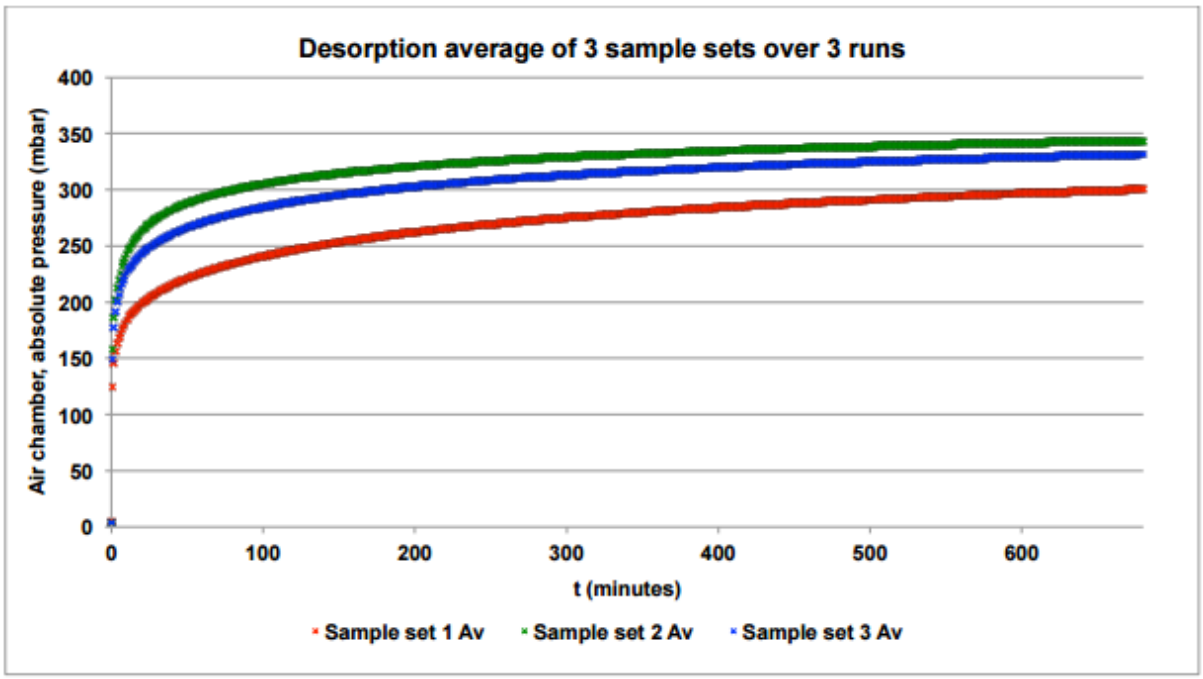

Figure 10: Desorption comparison of three sample sets with differing bulk densities.

The derived model [9] is based on classical solutions for heat transfer. Time dependent diffusion of gas or vapour through porous solids is described by Fick's second law. The equation is the same as Fourier's equation for transient conduction of heat in solids, if the diffusion coefficient (D) is replaced by thermal diffusivity k/ρc (relative storage capacity/density*specific heat), and the concentration (C) and hence pressure is replaced by temperature. The analysis generated desorption diffusion coefficients in the range of 106-189 x 10^{-9} m^2s^{-1} and absorption diffusion coefficients in the range of

178-300 x 10^{-9} m^2s^{-1}. Sorz and Heitz [14], and Yokota [15] have previously reported results in the range of 24000 x 10^{-9} m^2s^{-1} to 0.95 x 10^{-9} m^2s^{-1} respectively for diffusion coefficients in hardwood.

6 CONCLUSIONS

The fabric architecture can have a significant effect on resin flow in a monolithic laminate, and the consequent formation of voids. This potential for void-related defect formation is greatly increased due to the complex 3D flow in a cored laminate, particularly when using un-sealed end-grain balsa where the sap channels provide increased through-thickness flow channels. The chosen infusion strategy and materials selection are both vital considerations in reducing the formation of voids.

Experiments have been conducted to provide data on the pore space in core materials, the absorption/desorption rate of air, and a diffusion coefficient for end-grain balsa wood. This knowledge has been utilised to show that evacuated partially permeable core materials in resin infused panels can permit manufacture of panels with reduced or eliminated knit line defects.

ACKNOWLEDGEMENTS

The authors are grateful to the Engineering and Physical Sciences Research Council (EPSRC) and Vestas Technology, Newport IoW for funding through a CASE Studentship. Further thanks are due to Tomas Vronsky for access to facilities at Vestas, to Mansell Davies for mathematical guidance and to Gregory Nash, Roy Moate and Peter Bond for assistance with experiments.

REFERENCES

[1] M.A. Dawson and L.J. Gibson, Biomimetics: extending nature's design of thin-wall shells with cellular cores, Design and Nature III: Comparing Design in Nature with Science and Engineering, WIT Transactions on Ecology and the Environment, 2006, 87, 145-155.

[2] Heng Hu, Salim Belouettar, Michel Potier-Ferry and El Mostafa Daya, Review and assessment of various theories for modeling sandwich composites, Composite Structures, July 2008, 84(3), 282-292.

[3] S Malek and LJ Gibson, Multi-scale modelling of elastic properties of balsa, International Journal of Solids and Structures, available online 24 January 2017.

[4] SP Silva, MA Sabino, EM Fernandes, VM Correlo, LF Boesel and RL Reis, Cork: properties, capabilities and applications, International Materials Reviews, 01 December 2005, 50(6), 345-365.

[5] Carla Leite and Helena Pereira [117 references], Cork-containing barks - a review, Frontiers in Materials, 19 January 2017, 3(63), 1-19.

[6] C.D. Williams, J. Summerscales and S.M. Grove, Resin infusion under flexible tooling (RIFT): a review, *Composites Part A: Applied Science and Manufacturing*, **27A(7)**, 1996, 517-524 (doi: 10.1016/1359-835X(96)00008-5).

[7] J. Summerscales and T.J. Searle, Review: Low pressure (vacuum infusion) techniques for moulding large composite structures, *Proc IMechE Part L: Journal of Materials: Design and Applications*, **L219(1)**, 2005, 45-58 (doi: 10.1243/146442005X10238).

[8] J. Summerscales, Resin Infusion Under Flexible Tooling (RIFT), In *Encyclopedia of Composites – second edition*, (*Eds: L. Nicolais and A. Borzacchiello*, John Wiley & Sons, 2012, pp 2648-2658 (doi: 10.1002/9781118097298.weoc216).

[9] Richard Cullen, Air permeability of balsa core, and its influence on defect formation in resin infused sandwich laminates, PhD thesis, University of Plymouth, 2014. (hdl: 10026.1/2988).

[10] ISO 3130:1975 Wood - Determination of moisture content for physical and mechanical tests, International Organization for Standardization, Geneva, 1975.

[11] H.S. Carslaw and J.C. Jaeger, Conduction of Heat in Solids - second edition, Oxford University Press, Oxford, 1959.

[12] R.A.H. Pomeroy, Permeability characterisation of continuous filament mats for resin transfer moulding, PhD thesis, Plymouth University, 2009 (hdl: 10026.1/2691.

[13] J.M. Lawrence, V. Neascu and S.G. Advani, Modeling the impact of capillary pressure and air entrapment on fiber tow saturation during resin infusion in LCM, Composites Part A: Applied Science and Manufacturing, **40(8)**, August 2009, 1053-1064 (doi: 10.1016/j.compositesa.2009.04.013).

[14] J. Sorz and P. Heitz, Gas diffusion through wood: implications for oxygen supply, Trees, 2006, 34-41. 552 (doi: 10.1007/s00468-005-0010-x).

[15] T. Yokota, Diffusion of non-swelling gas through wood, Mokuzai Gakkaishi, 1967, **13(6)**, 225-231.